Two-dimensional Ising-like model with specific edge effects for spin-crossover nanoparticles: A Monte Carlo study

Azusa Muraoka,* Kamel Boukheddaden,† Jorge Linarès, and F. Varret
Groupe d'Etudes de la Matière Condensée (GEMAC), Université de Versailles Saint-Quentin-CNRS, 45 Avenue des Etats-Unis, 78035 Versailles, France
(Received 7 December 2010; revised manuscript received 9 June 2011; published 18 August 2011)

We analyzed the size effect of spin-crossover transition nanoparticles in a two-dimensional core-shell model, where the edge atoms are constrained to the high-spin (HS) state. Using Monte Carlo (MC) simulations, we showed that this specific edge effect lowers the equilibrium temperature and enhances the HS residual at low temperature; these results are in very good agreement with recent experimental data. Within a very simple working assumption, we obtained an analytical expression for the size dependence of the equilibrium temperature that is in excellent agreement with the MC results. The model leads to a nontrivial size dependence of the hysteresis width, which is similar to a—size-dependent—negative pressure effect induced by the HS edges. To reach the best agreement with experimental data, we accounted for the size distribution of the experimental samples.

DOI: 10.1103/PhysRevB.84.054119 PACS number(s): 78.67.Rb, 75.30.Wx, 75.75.Fk, 65.80.−g

I. INTRODUCTION

In recent years, there has been growing interest in the field of spin-crossover (SC) solids. Under various constraints, such as temperature[1] or pressure[2–4] variations, irradiation by visible light,[5–9] or magnetic field,[10] SC solids can be switched from a low-spin (LS) state to a high-spin (HS) state and vice versa.[11,12] For example, Fe^{II} SC compounds[13] are diamagnetic ($S = 0$, LS) and paramagnetic ($S = 2$, HS) in the low- and high-temperature phases, respectively. The spin-crossover transition involves both electronic transformation (spin and orbital) and structural modifications. In the case of Fe^{II} compounds, the metal-ligand bond lengths change by about 0.2 Å (∼10%), and the ligand-metal-ligand bond angles change by 0.5°–8°.[6,14] Optical properties are also changed,[5,15,16] with usually a colorless HS state and a strongly colored LS state in the case of Fe^{II} systems. Consequently, magnetic and optical measurements[17–20] are the major experimental techniques used for quantitative investigations of spin transitions. In many cases, elastic interactions between the SC units are strong enough to induce hysteresis at the thermal spin transition,[21] which occurs as a first-order phase transition. Such "switchable" molecular solids are promising in terms of optical data storage.[22]

Recently, the synthesis and design of spin-crossover nanoparticles have become possible, and several interesting behaviors have been reported.[23–33] The experimental results, for most of these studies, have confirmed the expected narrowing of hysteresis loop and, in some cases, the collapse of the loop below some "critical size," but very few of them have provided a coherent set of data over the relevant size range, that is, above and below the critical size. In addition, the samples usually present a rather wide distribution of sizes and various shapes, and particles are often aggregated in various manners. All these features obviously impact the switching behavior of the SC nanoparticles and make investigation into the properties of a unique nanoparticle a very challenging goal. From the theoretical point of view, there have been a few studies of the thermal and photo-switching properties of SC nanoparticles,[34–37] that have aimed at reproducing the collapse of the hysteresis effects at the critical size of the particles. These theoretical studies were based on Metropolis simulations on finite-size lattices with free boundary conditions. Here, we introduce an additional aspect, which is the specific electronic state of the atoms located at the surface of the particle. This was suggested by a recent experimental investigation[25] on SC nanoparticles of Fe(pyrazine){$Pt(CN)_4$}, with well-controlled sizes above and below the critical size. In addition to the expected narrowing of the hysteresis loop upon decreasing size, this system displayed a sizable lowering of the transition temperature and an increase of the residual HS fraction. The latter features are explained by the different coordination of the surface atoms, including water molecules instead of the organic ligands. These surface atoms experience a weaker ligand field capable of trapping them in the HS state, and consequently lower the equilibrium temperature of the particle through an effective negative pressure effect. For practical reasons, the present investigation was performed on two-dimensional (2-D) networks where this specific effect was located at the edges. It will be consequently referred to in terms of "edge effect." Although the present 2-D model might be considered as a preliminary approach to future three-dimensional (3-D) models, it is also relevant due to the particular geometry of the nanocrystals, which are in the shape of square platelets with a rather constant thickness. The core of the square lattice is already submitted to a quasi-uniform effect from both surfaces, irrespective of the size of the network, and the size effect effectively reduces to a 2-D problem. This viewpoint will be supported by the present simulations. We performed Monte Carlo (MC) simulations using the well-known Ising-like model (interacting two-level systems), which has been widely used in literature to describe the equilibrium[39,40] and nonequilibrium[41] properties of SC solids. This choice was dictated by the simplicity of this description, despite its phenomenological character. The paper is organized as follows: Sec. II is devoted to the model; Sec. III provides the results and their discussion; Sec. IV presents a detailed comparison to experimental data, including the impact of size distributions; and Sec. V is the conclusion.

II. MODEL

The total Hamiltonian of the system accounting for the edge effect is written

$$H = -J \sum_{(i,j)} \sum_{\substack{i'=\pm 1;\\ j'=\pm 1}} S(i,j)S(i+i', j+j') + \left(\frac{\Delta}{2} - \frac{k_B T}{2} \ln g\right) \sum_{(i,j)} S(i,j)$$

$$\text{and} \quad S(i,N) = S(N,j) = S(i,1) = S(1,j) = +1 \qquad (1)$$

In this Hamiltonian expression, the HS and LS states are associated, respectively, with the eigenvalues $+1$ and -1 of the fictitious spin operator, S, with their respective different degeneracies g_+ and g_-, the ratio of which is $\frac{g_+}{g_-} = g$. These degeneracies account for both internal (spin, orbit, and intermolecular vibrations) and external (lattice phonons) degrees of freedom. Here, Δ is the energy difference E(HS) $-$ E(LS) between the spin states of isolated molecules, and J is a phenomenological parameter accounting for ferroelastic interactions, here limited to first-neighbor molecules. The order parameter of the system is the HS fraction, defined as $n_{\mathrm{HS}} = (1 + \langle S \rangle)/2$, where

$$\langle S \rangle = \frac{4(L-1) + \sum_{i=1}^{(L-2)^2} S_i}{L^2}, \qquad (2)$$

where L^2 is the system size.

The equilibrium temperature, T_{eq}, is defined as the temperature for which the spin fractions are equal ($n_{\mathrm{HS}} = 1/2$). In the case of a first-order transition (for which the spin equilibrium is unstable), it is approximately equal to the mean value of the heating and warming transition temperatures, also defined by equal spin fractions on the heating and cooling branches of the hysteresis loop.

The present model involves various local situations, the features of which are listed in Table I. The key point is that the interaction terms associated with the presence of HS-fixed neighbors around a considered atom introduce fixed contributions to the energy gap, precisely $-J$ for each neighbor. These fixed contributions effectively act as ligand-field contributions and consequently have to be incorporated in the ligand-field term of the considered atom. In other words, they locally act as a negative pressure.

The Hamiltonian equation (1) was exactly solved in the canonical approach using Monte Carlo (MC) simulations based on the Metropolis algorithm.[42] Parameter values were chosen from typical data in spin-crossover literature, such as the molar entropy change $\Delta S \approx 50$ J/K/mol, leading to ln $g = \Delta S/\mathrm{R} \approx 6$ (where R is the perfect gas constant) and energy gap $\Delta = 1300$ K, leading to a typical value of the equilibrium temperature $T_{\mathrm{eq}} = \frac{\Delta}{k_B \ln g} \approx 200$ K. Comparison to experimental values is possible through adequate energy rescaling, that is, by considering relative temperature variations. Accordingly, the interaction parameter value $J = 160$ K was selected so as to result in a relative hysteresis width $\Delta T_c/T_{\mathrm{eq}} = (T_{\mathrm{c,up}} - T_{\mathrm{c,down}})/T_{\mathrm{eq}}$, which compares to the experimental value of the bulk system, $\approx 15/300$.

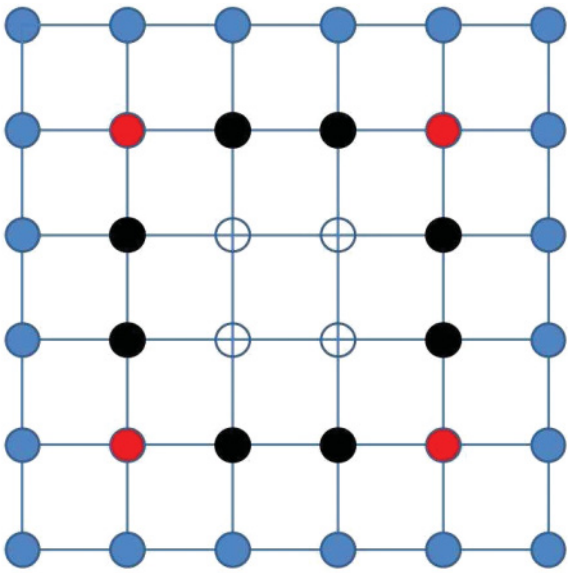

FIG. 1. (Color online) Lattice configuration in the case $L = 6$. Blue filled circles are HS-fixed (edge) atoms. All inside atoms are active: Filled red (black) circles stand for atoms having two (one) inactive HS as nearest-neighbors, and open circles stand for atoms surrounded by only active sites.

Simulations were performed on square lattices of size $L \times L$ (see Fig. 1), up to $L = 200$. Due to the fixed character of the edges, the usual criterion of open/periodic boundary conditions did not apply. To follow the thermal dependence of the HS fraction, $n_{\mathrm{HS}}(T)$, the system was warmed from $T = 50$ K to 250 K and cooled down to the initial temperature 50 K by 1 K steps. At each temperature, the first 20,000 MC steps were discarded, due to their transient regime character, and the following 100,000 MC steps were used for calculating the average physical quantities of the system at the quasi-equilibrium state. For each size, the process was repeated 20 times with different random seed generators, and the results were averaged.

TABLE I. The various situations and ligand-field contributions in an $L \times L$ lattice.

	Total	Edges	Core	Core, number of HS-fixed neighbors			
				0	1	2	4 for $L = 3$ only
Number of atoms	L^2	$4(L-1)$	$(L-2)^2$	$(L-4)^2$	$4(L-4)$	4	1
Ligand field				$\frac{\Delta}{2} - \frac{k_B T}{2} \ln g = A$	$A - J$	$A - 2J$	$A - 4J$

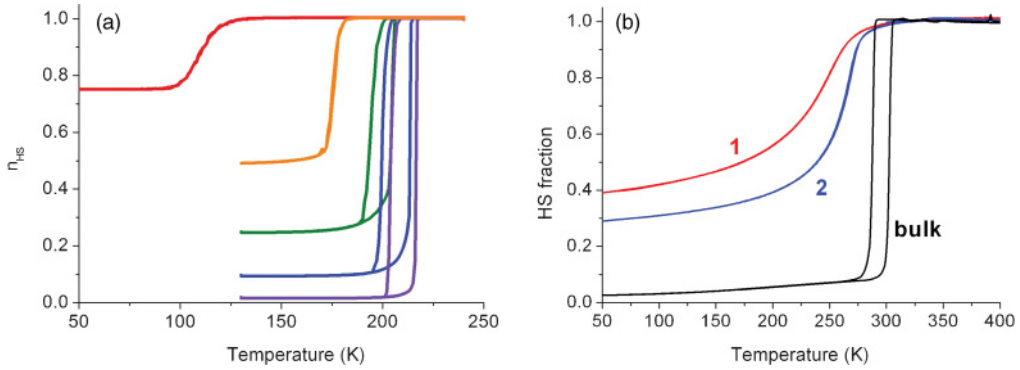

FIG. 2. (Color online) (a) Calculated thermal dependence of the HS fraction for square-shaped nanoparticles of different sizes. From left to right, $L = 4$, 7, 10, 40, 200 (quasi-infinity). (b) Experimental HS fraction (after Ref. 25) of the bulk and nanoparticle samples of the SC compound Fe(pyrazine){$Pt(CN)_4$}. Labels 1 and 2 stand for nanoparticle samples with mean size ∼7 nm and ∼12 nm, respectively.

III. RESULTS AND DISCUSSION

In Fig. 2, we show the thermal behavior of the HS fraction, $n_{\rm HS}(T)$, calculated for various particle sizes (Fig. 2(a)), and the experimental data (Fig. 2(b)) that inspired the work. The experimental behaviors are reproduced: Upon decreasing particle size, the transition temperature is shifted downward, the hysteresis loop progressively collapses, and the low-temperature residual HS fraction is increased. Detailed discussion of the results of the model follows.

A. Size dependence of the residual fraction and of the equilibrium temperature

The low-temperature HS residual fraction exactly follows the edges/core atom ratio, which is simply expressed as $\frac{4(L-1)}{L^2}$, with asymptotic regime $\sim 4/L$ for large nanoparticles (see Fig. 3(a)). The equilibrium temperature follows a power law $\sim (L-2)$ (see Fig. 3(b)), which outlines that the effective size of the system is $(L-2) \times (L-2)$, that is, the size of the SC-active core.

We found that the size dependence of the transition temperature could be described by analytical laws (easily extended to 3-D models). For small sizes, exact solutions are found, since all active atoms are described by identical Hamiltonians:

For $L = 2$: There is no spin-crossover transition by construction, since all 4 atoms are edge atoms.

For $L = 3$: The unique core atom results in a continuous behavior according to the canonical expression $n_{HS} = \frac{1+th\beta(4J-\frac{\Delta}{2}+\frac{k_BT}{2}\ln g)}{2}$, leading to $T_{\rm eq}(L=3) \approx 3$ K, with the present set of parameters.

For $L = 4$: Each of the 4 core atoms has two HS nearest neighbors. The effective ligand-field energy, $\frac{\Delta}{2} - \frac{k_BT}{2}\ln g - 2J$, is positive at 0 K, and hence the LS state is the ground state at 0 K. The canonical expression of the HS fraction is given by

$$n_{HS} = \frac{1}{8}\left\{7 - \frac{sh\beta\left(\frac{\Delta}{2} - 2J - \frac{k_BT}{2}\ln g\right)}{sh^2\beta\left(2J - \frac{\Delta}{2} + \frac{k_BT}{2}\ln g + \exp\left(-\frac{J}{k_BT}\right)\right)}\right\}. \quad (3)$$

Equation (3) leads to a continuous behavior with an equilibrium temperature $T_{\rm eq} = \frac{\Delta - 4J}{k_B \ln g} = 110$ K, which is in excellent agreement with that of MC simulations for $L = 4$, reported in Fig. 2(a).

For larger sizes, the lattice contains spin-crossover active spins with zero, one, or two HS-fixed neighbors. At the present state-of-art of the mathematical techniques, there is no analytical solution of this problem. We introduce here a simple solution based on the working assumption that

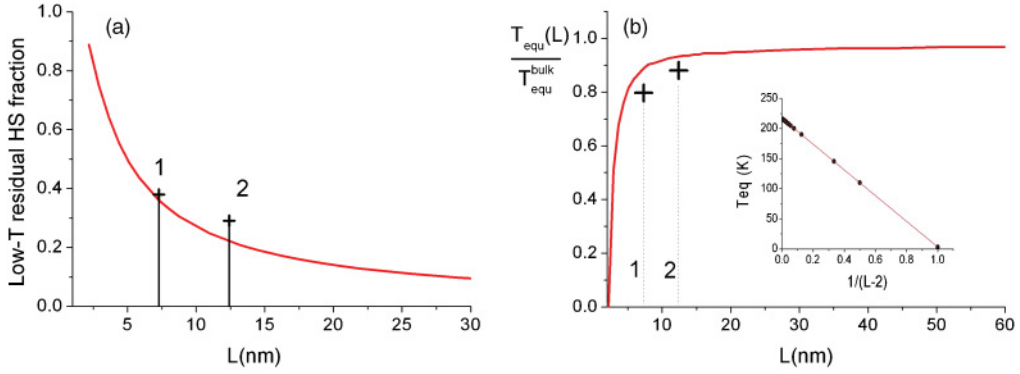

FIG. 3. (Color online) (a) The calculated size dependence of the residual HS fraction at low temperature (full line) compared to experimental data (+) derived from Fig. 2(b). (b) The calculated size dependence of the equilibrium temperature (full line), compared to experimental data (+) derived from Fig. 2(b). Inset: the validity check of the analytical Eq. (5).

the equilibrium temperature of the system results from the average value of the ligand fields. Taking advantage of the data listed on Table I, the transition temperature is expressed as:

$$T_{\mathrm{eq}}(L) = \frac{4 \times \frac{\Delta - 4J}{k_B \ln g} + [4(L-2) - 8] \times \left(\frac{\Delta - 2J}{k_B \ln g}\right) + (L-4)^2 \times \frac{\Delta}{k_B \ln g}}{(L-2)^2}. \quad (4)$$

Equation (4) can be rewritten in a more adequate form as

$$T_{\mathrm{eq}}(L) = T_{\mathrm{eq}}(\infty) - \frac{8J}{k_B \ln g} \times \frac{1}{L-2}, \quad (5)$$

where $T_{\mathrm{eq}}(\infty) = \frac{\Delta}{k_B \ln g} \approx 216$ K is the transition temperature of the infinite system, and the second term, $-\frac{8J}{k_B \ln g} \times \frac{1}{L-2}$, expresses the size dependence introduced by the HS-fixed edges.

The relevance of Eq. (5) is supported by the comparison to the results of the MC simulations, as shown in the inset of Fig. 3(b), where T_{eq} is plotted vs $1/(L-2)$. The linear regression of the MC data yields a slope value -210 ± 4 K, which is in excellent agreement with the analytical prediction $-\frac{8J}{k_B \ln g} \sim -213$ K.

It is worth mentioning that the latter method also holds for a 3-D cubic system. A general formula for the evolution of the equilibrium temperature with size is given by

$$T_{\mathrm{eq}}(L) = T_{\mathrm{eq}}(\infty) - \frac{4dJ}{k_B \ln g} \times \frac{1}{L-2}, \quad (6)$$

where d is the dimensionality of the system.

We should also mention that the present model involves the assumption that the effective degeneracy g is constant. Thus, g is not affected by the edge effect and does not depend on the particle size. The first assumption is inherent to the Ising-like model itself, which uses HS and LS g values irrespective of the spin state of the neighbors. The second assumption is worth being questioned: On one hand, the orbital and spin degeneracies, which have discrete values, can easily be assumed to be size independent; on the other hand, the intramolecular vibration frequencies as well as the phonons density of states—including surface and edge effects—might be affected by the nanoparticle size. This problem cannot be addressed at the present time, in absence of experimental data by infrared (IR) and/or Raman spectroscopy, which so far are missing in the case of SC nanoparticles. We just believe that the dispersion curves of surface atoms and bulk atoms should be different,[43–45] due to the impact of surface relaxation and to the existence of specific defects at the surface. Accounting for these aspects would require using lattice dynamics models, which were not in the scope of the present work.

B. On the size dependence of the hysteresis loop

According to Fig. 2, the hysteresis loop appears above a threshold value, $L_{\mathrm{thresh.}} \sim 7$–8. This value certainly depends on the MC kinetics used in the simulation, which will be kept constant throughout the present work. It is worth noting that the spatial scale of the model is easily determined from the measured Fe-Fe distance, ~ 0.72 nm in the dense planes of the structure.[46] On the contrary, the timescale of MC can hardly be compared to the experimental switching times, which usually are in the microsecond range for isolated atoms at the considered temperatures, but which are very efficiently increased at the vicinity of the transition.[47] We merely assumed that both experimental and thermal calculated data correspond to a quasistatic hysteresis, that is, they belong to a regime that does not sizably depend on the temperature sweep rate.

We reported in Fig. 4 the size dependence of the hysteresis width. On increasing size, above some critical value ($L_c \sim$ 7–8), ΔT_C shows a monotonous increase up to a peak value at $L \sim 24$–25 and then slightly decreases towards an asymptotic value, which sizably differs from that of the free-edge system. This nonmonotonic behavior contrasts with the monotonic behavior of free border nanoparticles, also reported in Fig. 4.

The variation of ΔT_C (L) above the peak value can be assigned to the variation of T_{eq}, under the nontrivial size-dependent "pressure effect"[48] of HS-fixed edges, which remains sizeable while the effective interactions in the system have almost reached their asymptotic values. It is well known, indeed, from the phase diagram of the Ising-like system, that increasing T_{eq} while keeping constant the interaction parameter leads to a decrease in the hysteresis width.[40] In other words,

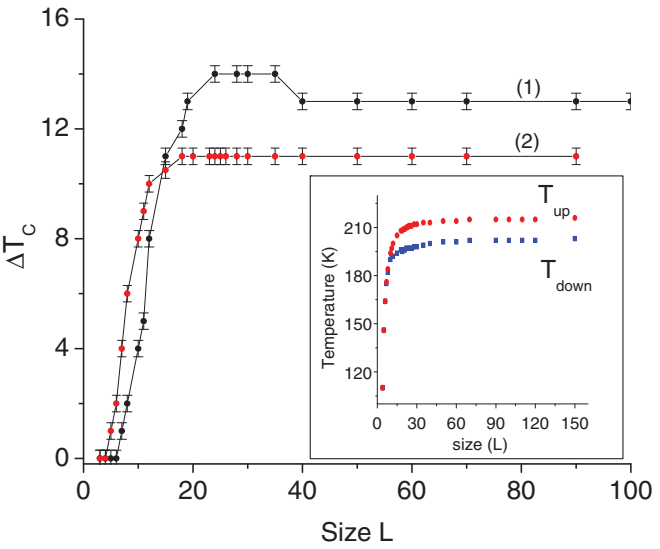

FIG. 4. (Color online) The calculated size dependence of the width of thermal hysteresis, ΔT_C , for fixed HS boundary condition (curve 1) and free boundary condition (curve 2). Inset: the size-dependence of the transition temperatures upon heating (T_{up}) and cooling (T_{down}) corresponding to curve (1).

this nonmonotonous behavior results from the competition of two parameters affected by the size effect: the equilibrium temperature and the effective cooperativity of the system.

To find supporting evidence for this mechanism, we performed MC simulations without specific surface effects (free boundary conditions) and calculated the size dependence of the hysteresis width for the same MC kinetics. The results, shown in Fig. 4, together with those of fixed boundary conditions, confirm the present analysis. To our best knowledge, this nonmonotonic behavior is a new result in the field of SC and makes desirable the achievement of detailed experiments devoted to size effects.

In the present discussion, we did not address the kinetics aspects involved in the observation of the hysteresis loop. We previously investigated in detail, some years ago,[44] the lifetime of the metastable states of the Ising-like model. The results showed that a decrease in the size of the systems resulted in a decrease of the lifetime of the metastable states around the first-order transition; in contrast, decreasing the ligand field (as produced by the negative pressure) induced the opposite effect. The possible balance between these opposite effects is an open question, which will be investigated quantitatively in a forthcoming paper making use of the absorbing Markov chain method, following Lee *et al.*[49]

We briefly considered the possible impact of long-range interactions at the intraparticle, which actually are of elastic nature in spin-crossover systems. Calculations showed that such intraparticle interactions may hinder the appearance of the nonmonotonic behavior reported here. This tendency can be easily understood by considering the case of pure infinite long-range interactions for which the system loses morphology (the location of the HS atoms at the surface or in the bulk is pointless) and consequently surface effects vanish. In contrast, introducing interactions at interparticle levels is an open problem in the case of spin-crossover systems, for which no equivalent to the magnetic dipolar interaction is known at the present time.

In both situations (intra- or interparticles interactions), the major consequence of long-range interactions is a decrease in the critical size of bistability.

C. On the occurrence of the first-order transition

The case of infinite 2-D networks has been previously described using the present Ising-like approach with first-neighbor interactions.[19] The occurrence condition of the first-order transition is $T_C^\infty > T_{eq}$, where $T_C^\infty = 2{,}269J$ is the order-disorder transition of the pure 2-D Ising model (without field and degeneracy), and $T_{eq} = \frac{\Delta}{k_B \ln g}$ is the equilibrium temperature of the Ising-like system, irrespective of the interaction strength. At finite size, the equilibrium transition temperature of the usual Ising-like system (that is, with free boundary conditions) is size independent, while the order-disorder transition $T_C(L)$ strongly depends on size as already reported in literature.[50] Indeed, for the finite 2-D Ising model with periodic boundary conditions, algebraic analysis made by Ferdinand and Fisher[51] showed that for an $L \times L$ system, the specific heat was rounded with a maximum at a temperature T_m, the so-called "quasicritical temperature," which is shifted with respect to T_C^∞ (the critical temperature of the infinite lattice) so that,

$$\left|T_m - T_C^\infty\right| / T_C^\infty \propto 1/L. \tag{7}$$

Monte Carlo simulations realized on 2-D (pure) Ising systems[26] have shown $T_m > T_C^\infty$. Thus, applying naively the previously said occurrence condition necessarily yields $T_m > T_{eq}$ as soon as $T_C^\infty > T_{eq}$. The latter condition apparently disagrees with the fact that the first-order transition is lost under some critical size. This can be explained by considering the criticality of the transition of the (2-D) pure Ising model, which strongly decreases upon decreasing size.[52,53] In other words, the order-disorder transition of the pure Ising model, needed for the presence of the first-order transition of the Ising-like model, vanishes at small sizes.

D. Size distribution effects

SC nanoparticle samples usually involve size distributions, which are easily accounted for in the frame of the present model. Here, we use size distributions determined in Ref. 25 from transmission electron microscopy (TEM) images (see Fig. 5). The intermolecular distance, measured in the HS state, ∼1 nm, defines the actual scale of the model. We consider here two samples with sizably different average sizes, ∼7 and 12 nm.

Let's denote $P(L)$ the probability density of finding a square-shaped nanoparticle with edge size L. Since the HS fraction is a volume response, the average HS fraction over

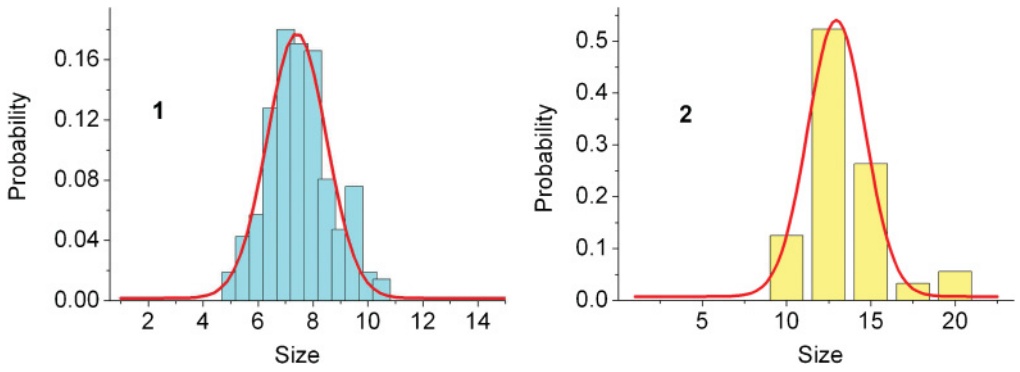

FIG. 5. (Color online) Experimental size distributions of the nanoparticle samples, with best Gaussian fits (after Ref. 25).

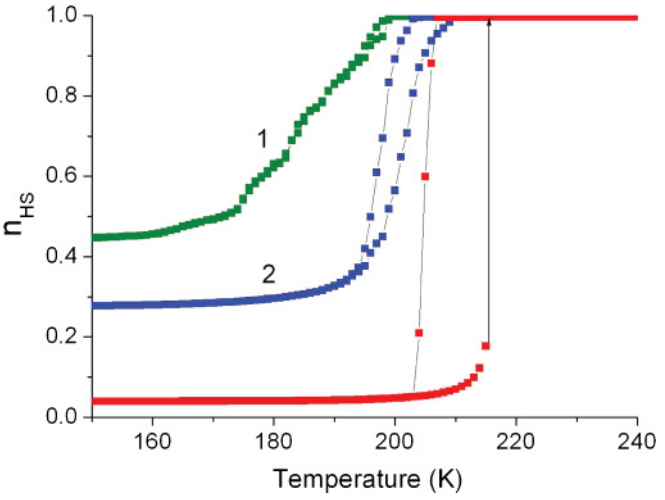

FIG. 6. (Color online) Calculated thermal variation of the HS fraction resulting from the size distributions shown in Fig. 5. The bulk curve (right curve) was calculated in the absence of distribution.

the different nanoparticles is given by

$$n_{HS}(T) = \frac{\int_0^\infty P(L) \times dL \times n_{HS}(L,T) \times V}{\int_0^\infty P(L) \times dL \times V}, \qquad (8)$$

where the volume V is taken proportional to L^2, because particles thickness is approximately constant.

Simulations were performed with MC kinetics already used in the previous section, and with identical values of thermodynamic parameters. The results are reported in Fig. 6, and they qualitatively agree with the experimental data: The 7 nm centered distribution displays a gradual transition, while the 12 nm one displays a first-order transition with a narrow and bent hysteresis loop. In both cases, however, the average equilibrium temperatures are larger than those of the individual nanoparticles of same size. This can be explained by the weighting factor V in Eq. (7), which enhances the response of the larger particles. It is worth mentioning that the reverse problem, that is, analyzing the experimental response of a set of size-distributed particles, can be solved by using the FORC technique (first-order reversal curves).[33]

It is interesting to mention that the residual HS fraction at 0 K, briefly discussed in the introduction of Sec. III, the size dependence of which is given by $\frac{4(L-1)}{L^2}$ in the case of a single square-shaped nanoparticle of size L, can be also derived for an ensemble of size-distributed nanoparticles using Eq. (7). This can be written

$$n^0_{HS} = \frac{4\int_0^\infty P(L) \times dL \times (L-1)}{\int_0^\infty P(L) \times dL \times L^2}. \qquad (9)$$

To understand the impact of the size distribution on the residual HS fraction, we use a Gaussian distribution for $P(L)$, so that $P(L) = \frac{1}{\sigma\sqrt{2\pi}} e^{\frac{(L-\bar{L})^2}{2\sigma^2}}$. Simple calculus leads in such a case to the following expression for the residual fraction:

$$n^0_{HS} = \frac{4(\bar{L}-1)}{(\overline{L^2})}, \quad \text{where} \quad \overline{L^2} = (\bar{L})^2 + \sigma^2, \qquad (10)$$

in which the dispersion of the distribution appears clearly in the resulting residual fraction. Although Eq. (9) depends on the shape of the particles, it is interesting to note that a deep inspection of the evolution of the residual HS fraction (usually obtained from magnetic data) may lead to relevant statistical information on the particle distribution and vice versa.

IV. CONCLUSION

The impact of specific conditions at the edges of the 2-D model has been investigated. The choice of HS-fixed edges was based on the observation of an increasing residual HS fraction at low temperature, upon particle size reduction. This specific boundary condition basically acts as a negative pressure, which shifts the equilibrium temperature downward in a size-dependent way. The interplay between this equilibrium temperature variation and the expected variation of the effective interactions in the system leads to a nonmonotonous dependence of the width of the hysteresis loop upon the particle size. The main experimental features of nanoparticle samples of the compound Fe(pyrazine){$Pt(CN)_4$} are rather well reproduced by the present model. We also described the way in which the usual occurrence condition of the first-order transition has to be adapted to the nanoscale.

Further aspects related to the nanoparticle problem remain to be explored: the introduction of more realistic surface effects through core-shell models with explicit dependence of the ligand field, for example, and the impact of nanoparticle morphology. Our first simulations using circular-shaped nanoparticles did not show significant differences with respect to the square-shaped ones investigated here. This is presumably due to the roughness of the boundary introduced by the discrete nature of the lattice. The problem is under investigation.

ACKNOWLEDGMENTS

The present work has been supported by the University of Versailles, Centre National de la Recherche Scientifique (CNRS), Groupement de Recherche International (GDRI) France-Japan, and Pôle de Recherche et d'enseignement Supérieur (PRES-UniverSUd) Commutation aux petites échelles Spatiales (COPECS) project. The authors are indebted to S. Miyashita for helpful discussions and to Talal Mallah for providing the experimental data. Dr. A. Muraoka acknowledges University of Versailles St-Quentin for financial support.

*Present address: Meiji University, 1-1-1 Higashimita, Tama-ku, Kawasaki Kanagawa 214-8571, Japan.
†Corresponding author: kbo@physique.uvsq.fr

[1] P. Gütlich, Struct. Bonding, Berlin **44**, 83 (1981).
[2] O. Kahn and J. P. Launay, Chemtronics **3**, 140 (1988).
[3] J. Jeftic and A. Hauser, J. Phys. Chem. B **101**, 10262 (1997).

[4]G. Molnár, V. Niel, J.-A. Real, L. Dubrovinsky, A. Bousseksou, and J. McGarvey, J. Phys. Chem. B **107**, 3149 (2003).
[5]S. Decurtins, P. Gütlich, C. P. Köhler, H. Spiering, and A. Hauser, Chem. Phys. Lett. **105**, 1 (1984).
[6]P. Gütlich, A. Hauser, and H. Spiering, Angew. Chem., Int. Ed. Engl. **33**, 2024 (1994).
[7]S. Bonhommeau, G. Molnár, A. Galet, A. Zwick, J.-A. Real, J. J. McGarvey, and A. Bousseksou, Angew. Chem., Int. Ed. **44**, 4069 (2005).
[8]N. O. Moussa, G. Molnár, S. Bonhommeau, A. Zwick, S. Mouri, K. Tanaka, J. A. Real, and A. Bousseksou, Phys. Rev. Lett. **94**, 107205 (2005).
[9]S. Decurtins, P. Gütlich, K. M. Hasselbach, A. Hauser, and H. Spiering, Inorg. Chem. **24**, 2174 (1985).
[10]A. Bousseksou, K. Boukheddaden, M. Goiran, C. Consejo, M.-L. Boillot, and J.-P. Tuchagues, Phys. Rev. B **65**, 172412 (2002).
[11]E. König, Struct. Bonding Berlin **76**, 51 (1991).
[12]O. Kahn, Curr. Opin. Solid State Mater. Sci. **1**, 547 (1996).
[13]J. Krober, E. Codjovi, O. Kahn, F. Grolière, and C. Jay, J. Am. Chem. Soc. **115**, 9810 (1993).
[14]B. Gallois, J.-A. Real, C. Hauw, and J. Zarembowitch, Inorg. Chem. **29**, 1152 (1990).
[15]E. W. Müller, J. Ensling, H. Spiering, and P. Gütlich, Inorg. Chem. **22**, 2074 (1983).
[16]G. Vos, R. A. Le Fèbre, R. A. G. de Graff, J. G. Haasnoot, and J. Reedijk, J. Am. Chem. Soc. **105**, 1682 (1983).
[17]E. König, G. Ritter, S. K. Kulshreshtha, J. Waigel, and H. A. Goodwin, Inorg. Chem. **23**, 1896 (1984).
[18]E. König, G. Ritter, H. Grünsteudel, J. Dengler, and J. Nelson, Inorg. Chem. **33**, 837 (1994).
[19]V. Ksenofontov, H. Spiering, A. Schreiner, G. Levchenko, H. A. Goodwin, and P. Gütlich, J. Phys. Chem. Solids **60**, 393 (1999).
[20]A. Bousseksou, G. Molnár, P. Demont, and J. Mengotto, J. Mater. Chem. **13**, 2069 (2003).
[21]O. Kahn, *Molecular Magnetism* (VCH, New York, 1993).
[22]O. Kahn, J. Krober, and C. Jay, Adv. Mater. Weinheim, Ger. **11**, 4 (1992).
[23]E. Coronado, J. R. Galán-Mascarós, M. Monrabal-Capilla, J. García-Martínez, and P. Pardo-Ibáñez, Advan. Mat. **19**, 1359 (2007).
[24]T. Forestier, S. Mornet, N. Daro, T. Nishihara, S. Mouri, K. Tanaka, O. Fouché, and E. Freysz Jean-François Létard, Chem. Commun. 4327 (2008).
[25]F. Volatron, L. Catala, E. Rivière, A. Gloter, O. Stephan, and T. Mallah, Inorg. Chem. **47**, 6584 (2008).
[26]I. Boldog, Ana B. Gaspar, V. Martinez, P. Pardo-Ibanez, V. Ksenofontov, A. Bhattacharjee, P. Gutlich, and José A. Real, Angew. Chem. **120**, 6533 (2008).
[27]T. Forestier, A. Kaiba, S. Pechev, D. Denux, P. Guionneau, C. Etrillard, N. Daro, E. Freysz, and J.-F. Létard, Chem. Europ. J. **15**, 6122 (2009).
[28]L. Catala, F. Volatron, D. Brinzei, and T. Mallah, Inorg. Chem. **48**, 3360 (2009).
[29]J. R. Galàn-Mascaros, E. Coronado, A. Forment-Aliaga, M. Monrabal-Capilla, E. Pinilla-Cienfuegos, and M. Ceolin, Chem. Mat. **22**, 4271 (2010); J. R. Galàn-Mascaros, E. Coronado, A. Forment-Aliaga, M. Monrabal-Capilla, E. Pinilla-Cienfuegos, and M. Ceolin, Inorg. Chem. **49**, 5706 (2010).
[30]C. Thibault, G. Molnar, L. Salmon, A. Bousseksou, and C. Vieu, Langmuir **26**, 1557 (2010).
[31]V. Martînez, I. Boldog, A. B. Gaspar, V. Ksenofontov, A. Bhattacharjee, P. Gùtlich, and J. A. Real, Chem. Mater. **22**, 4271 (2010).
[32]A. Tissot, J.-F. Bardeau, E. Rivière, F. Brisset, and M.-L. Boillot, Dalton Trans. **39**, 7806 (2010).
[33]A. Rotaru, F. Varret, A. Gindulescu, J. Linares, A. Stancu, J. F. Létard, T. Forestier, and C. Etrillard, Eur. Phys. J. B. (in revision).
[34]T. Kawamoto and S. Abe, Chem. Commun. 3933 (2005).
[35]T. Kawamoto and S. Abe, J. Phys. Condens. Matter **21**, 56 (2005).
[36]W. Nicolazzi, S. Pillet, and C. Lecomte, Phys. Rev. B **78**, 174401 (2008).
[37]Y. Konishi, H. Tokoro, M. Nishino, and S. Miyashita, Phys. Rev. Lett. **100**, 067206 (2008).
[38]C. Enachescu, L. Stoleriu, A. Stancu, and A. Hauser, Phys. Rev. Lett. **102**, 257204 (2009).
[39]J. Wanjflasz and R. Pick, J. Phys. Colloq. **32**, C1–91 (1971).
[40]A. Bousseksou, J. Nasser, J. Linarès, K. Boukheddaden, and F. Varret, J. Physique **2**, 1403 (1992).
[41]K. Boukheddaden, I. Shteto, B. Hôo, and F. Varret, Phys. Rev. B **62**, 14796 (2000).
[42]N. Metropolis, A. W. Rosenbluth, M. N. Rosenbluth, A. H. Teller, and E. Teller, J. Chem. Phys. **21**, 1087 (1953).
[43]J. Szeftel, Surf. Sci. **152-153**, 797 (1985).
[44]F. W. de Wette, in *Surface Phonons*, edited by W. Kress and F. W. de Wette (Springer-Verlag, Berlin, 1991).
[45]P. Brüesch, *Phonons: Theory and Experiments I: Lattice Dynamics and Models of Interatomic Forces* (Springer-Verlag, Berlin, 1982).
[46]V. Niel, J. M. Martinez-Agudo, M. Carmen Munoz, A. B. Gaspar, and J. A. Real, Inorg. Chem. **40**, 3838 (2001).
[47]I. Shteto, K. Boukheddaden, and F. Varret, Phys. Rev. E **60**, 5139 (1999).
[48]Pressure, p, favors the low-spin state due to its smaller volume and shifts upward the transition temperature according to Clapeyron's relation $\frac{dT}{dp} = \frac{\Delta V}{\Delta S}$, where ΔV and ΔS are the volume and entropy changes at the transition, respectively. Pressure usually results in a decrease of the width of the thermal hysteresis loop, which is explained through the usual two-level models in the assumption of a constant interaction parameter.
[49]J. Lee, M. A. Novotny, and P. A. Rikvold, Phys. Rev. E **52**, 356 (1995).
[50]H. C. Bolton and C. H. J. Johnson, Phys. Rev. B **13**, 3025 (1976).
[51]A. E. Ferdinand and M. Fisher, Phys. Rev. B **185**, 832 (1969).
[52]H. C. Bolton and D. W. R. Gruen, Phys. Rev. B **15**, 4544 (1977).
[53]C.-P. Yang, Am. Math. Soc. **15**, 351 (1963).